

Commercial Vehicle Braking Optimization: A Robust SIFT-Trajectory Approach

Zhe Li^{1,2} [†], Kun Cheng^{1,2} [†] ^{*}, Hanyue Mo^{1,2}, Jintao Lu^{1,2}, Ziwen Kuang^{1,2}, Jianwen Ye^{1,2}, Lixu Xu^{1,2}, Xinya Meng^{1,2}, Jiahui Zhao^{1,2}, Shengda Ji^{1,2}, Shuyuan Liu^{1,2}, and Mengyu Wang^{1,2}

¹ College of Information Engineering, China Jiliang University, No. 258 Xueyuan Street, Hangzhou, 310018, Zhejiang, China

² Zhejiang-New Zealand Joint Laboratory on Vision-Based Intelligent Metrology, China Jiliang University, Hangzhou 310018, China

Abstract. A vision-based trajectory analysis solution is proposed to address the "zero-speed braking" issue caused by inaccurate Controller Area Network (CAN) signals in commercial vehicle Automatic Emergency Braking (AEB) systems during low-speed operation. The algorithm utilizes the NVIDIA Jetson AGX Xavier platform to process sequential video frames from a blind spot camera, employing self-adaptive Contrast Limited Adaptive Histogram Equalization (CLAHE)-enhanced Scale-Invariant Feature Transform (SIFT) feature extraction and K-Nearest Neighbors (KNN)-Random Sample Consensus (RANSAC) matching. This allows for precise classification of the vehicle's motion state (static, vibration, moving). Key innovations include 1) multiframe trajectory displacement statistics (5-frame sliding window), 2) a dual-threshold state decision matrix, and 3) OBD-II driven dynamic Region of Interest (ROI) configuration. The system effectively suppresses environmental interference and false detection of dynamic objects, directly addressing the challenge of low-speed false activation in commercial vehicle safety systems. Evaluation in a real-world dataset (32,454 video segments from 1,852 vehicles) demonstrates an F1 score of 99.96% for static detection, 97.78% for moving state recognition, and a processing delay of 14.2 milliseconds (resolution 704×576). The deployment on-site shows an 89% reduction in false braking events, a 100% success rate in emergency braking, and a fault rate below 5%.

Keywords: Zero-Speed Detection · Automatic Emergency Braking · Low-Speed False Activation · Commercial Vehicle Safety · Vision-Based

1 Introduction

Between 2016 and 2017, Great Britain recorded approximately 174,510 road casualties, including 27,010 fatalities or serious injuries ([9]). The US Department of Transportation reports that more than 90% of traffic accidents are the

^{*} Corresponding author. E-mail: chengkun@ustc.edu

[†] These authors contributed equally to this work.

result of driver errors ([26]). Connected and Automated Vehicles (CAVs) have transformative potential to improve driving safety, traffic flow efficiency, and energy consumption optimization ([5]). As a critical active safety system, Automatic Emergency Braking (AEB) plays an important part in obstacle avoidance maneuvers ([36]). But its practical application in commercial vehicles faces a persistent technical challenge: misactivation at low speeds (particularly in the range of 0-5 km/h), significantly compromising the reliability of the system and user acceptance ([31]).

AEB operational logic is based on multiple decision criteria, with vehicle speed being the paramount. However, current implementations depend on Controller Area Network (CAN) signals that exhibit inherent precision limitations. This serial bus communication protocol, originally developed by Robert Bosch GmbH ([22]), facilitates data exchange between ECUs but struggles to accurately represent velocities in the critical range of 0-5 km/h. The resulting "zero-speed braking" phenomenon occurs when erroneous CAN readings trigger unnecessary full brake applications despite actual vehicle motion.

Existing solutions for zero-speed detection primarily fall into two categories: velocity-based methods and Inertial Measurement Unit (IMU)-sensor fusion approaches ([14,3,28]). This study introduces a cost-effective vision-based zero-speed detection algorithm as either a complementary or alternative solution. Leveraging blind-spot camera feeds, the proposed methodology employs adaptive feature analysis of sequential video frames to determine actual vehicle motion states. By integrating with the existing AEB decision pipeline through an auxiliary verification module, the system selectively suppresses unnecessary braking interventions only when true static conditions (including vibratory states) are confirmed, while maintaining robustness against environmental confounders such as illumination variations, precipitation, and dynamic object intrusions (e.g., pedestrians, vehicles).

Key innovations of this research include:

1. **Multi-frame trajectory displacement statistics:** Employing a 5-frame sliding window for temporal motion consistency analysis
2. **Adaptive CLAHE-SIFT feature enhancement:** Combining contrast normalization with scale-invariant feature extraction
3. **Dual-threshold state classification matrix:** Enabling precise differentiation between static/vibratory/moving states
4. **OBD-II-integrated dynamic ROI configuration:** Optimizing computational efficiency through region-of-interest adaptation

2 Related Work

2.1 Limitations of traditional AEB speed detection

The IMU sensor solutions ([3,28]) improved accuracy through acceleration compensation but suffered from vibration misjudgment, where engine idle vibrations

were often mistakenly identified as motion. This study, for the first time, distinguishes between vibration and actual motion through visual trajectory displacement statistics, achieving an F1 score of 96.40% (Figure III) for vibration state detection.

2.2 Development of Visual Motion Detection

The Scale-Invariant Feature Transform (SIFT) algorithm, proposed by David Lowe in 1999 and improved in 2004, extracts local feature descriptors that are invariant to scale, rotation, and illumination by constructing a difference-of-Gaussian pyramid and employing an extremum detection mechanism. It has become one of the most influential classic algorithms in the field of computer vision ([33,16,15,34]). In the field of vehicle dynamics analysis, SIFT features are widely applied in core tasks such as motion estimation, target tracking, and multi-modal data fusion, owing to their unique robustness. Feature-based methods dominate vehicle motion analysis. Research ([33]) indicates that Lowe's SIFT provides scale invariance but suffers from slow retrieval speeds and poor performance. This study utilizes Contrast Limited Adaptive Histogram Equalization (CLAHE) to enhance the feature quality of low-contrast scenes and integrates CLAHE-SIFT, which adaptively enhances contrast in low-light conditions, thereby improving the success rate of feature matching.

2.3 Challenges in Commercial Vehicle Scenarios

Commercial vehicles face more severe environmental conditions compared to passenger vehicles. Research ([23]) indicates that harsh weather conditions, such as rain and snow, can affect the accuracy of vision-based detection methods. Subsequent studies ([8,18]) have improved robustness by integrating radar and cameras, but this approach increases costs. Our solution employs a dynamic ROI (Region of Interest) filtering mechanism to exclude non-road areas (e.g., truck side mirrors), thereby reducing unnecessary computations.

2.4 Innovative positioning

TABLE 1 compares the intergenerational differences between this scheme and existing technologies.

3 Methodology

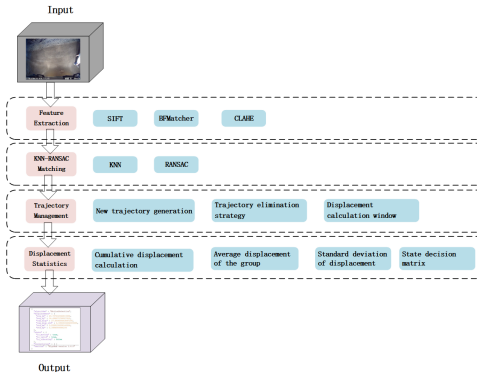
3.1 Overall Framework

The core algorithm framework of the system is shown in Figure 1. The general workflow of the algorithm is as follows: The system receives real-time video streams from the blind spot camera as input. Scale-Invariant Feature Transform (SIFT), Binary Feature Matching (BFMatcher), and Contrast Limited Adaptive

Table 1. Technical Solution Comparison Table

Technical Dimension	Existing Solution	Our Innovation
Feature Extraction	Baseline SIFT	CLAHE-SIFT + Dynamic ROI
State Classification	Binary (Moving/Static)	Ternary (Static/Vibration/Moving)
Hardware	IMU+GPU Fusion	Monocular Camera + Edge Computing

Histogram Equalization (CLAHE) are employed to enhance image features. A Region of Interest (ROI) is defined to filter out irrelevant areas and reduce environmental interference. The feature points extracted by SIFT are then matched using the K-Nearest Neighbors (KNN) algorithm ([25]), followed by verification through the Random Sample Consensus (RANSAC) algorithm to improve the accuracy and robustness of the matching process. Finally, through trajectory management and displacement statistics, the state of motion (static / vibrating / moving) is intelligently determined, and the result is packaged in JSON format, as shown in Figure 2, for the final output.

**Fig. 1.** Image Input to Output Processing Flow

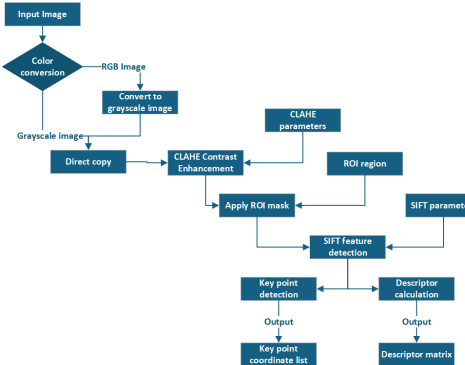
3.2 Feature Extraction

Feature extraction (Figure 3), as one of the most important steps in image classification, can capture a certain visual attribute of the image ([2]). Convert RGB images to grayscale when importing images to reduce computational complexity. Before feature detection, CLAHE (using an 8×8 grid histogram) is employed to enhance low-contrast regions. Dynamically set the focus area (top 5% to bottom 90%, left 15% to right 86%) through the ROI configuration file and adjust

```
{
  "algorithm" : "MotionDetection",
  "displacement" : {
    "avg_dx" : 23.707632064819336,
    "avg_dy" : 14.696975708007812,
    "cum_disp" : 27.893600463867188,
    "cum_disp_std" : 6.5953593254089355,
    "std_dx" : 3.8589158058166504,
    "std_dy" : 5.3486008644104
  },
  "state" : {
    "is_moving" : true,
    "is_valid" : true,
    "is_vibrating" : false
  },
  "trajectories" : [ {
    "version" : "AlgoHub version 1.4.0"
  }
}
```

Fig. 2. Output JSON

the actual size according to the installation requirements. In the Scale Invariant Feature Transform (SIFT) algorithms ([16,6]), we set an upper limit of 1000 feature points to control computational complexity, a contrast threshold of 0.04 to filter out low-contrast noise points, and an edge response threshold of 15.0 to exclude edge instability points; when there is blur, high noise, or uneven lighting in the image, it is necessary to dynamically adjust the contrast threshold and edge threshold to enhance robustness.

**Fig. 3.** Feature extraction module flowchart

3.3 Trajectory Management

Trajectory management involves four stages: creation, update, elimination, and reset. The system uses a 5-frame sliding window to maintain trajectories and determine states. The main technical implementation is as follows:

1. **Creation Mechanism:** When new feature points are successfully matched through KNN and RANSAC, the system assigns a unique ID to each point and initializes a trajectory queue, recording the initial position and the matching points of the current frame.
2. **Update Rule:** A sub-pixel level matching strategy is applied. Suppose the deviation between the current frame's matching points and the endpoint of the previous frame's trajectory is less than 1 pixel. In that case, the current point is appended, and the oldest position at the queue's head is cleared.
3. **Trajectory Elimination Mechanism:** After processing each frame, if a trajectory has not matched in the two consecutive frames, it is immediately discarded. This mechanism effectively removes invalid trajectories caused by brief occlusions or mismatches.
4. **Sliding Window:** The system uses a 5-frame sliding window (kWindowSize=5) for trajectory updates and state determination, ensuring real-time and accurate trajectory management.

3.4 Displacement statistics stage

Cumulative displacement calculation For each valid trajectory, this study calculated the displacement vector between its starting point (earliest position) and endpoint (latest position). The specific calculation method is as follows.

$$s = \sqrt{(x_i^{(end)} - x_i^{(start)})^2 + (y_i^{(end)} - y_i^{(start)})^2} \quad (1)$$

Afterwards, collect displacement data from all valid trajectories and calculate two core statistics.

Average displacement of the group The group average displacement is based on the matching results of feature points between consecutive frames and evaluates the motion state of vehicles by calculating the displacement of feature points on the image plane. The specific calculation formula is as follows:

$$\Delta dt = \frac{1}{n} \sum_{i=1}^n \sqrt{(x_i^{(end)} - x_i^{(start)})^2 + (y_i^{(end)} - y_i^{(start)})^2} \quad (2)$$

Among them, n represents the total number of valid trajectories. X_j^{end} and Y_j^{end} respectively represent the X and Y coordinates of the endpoint of the jth trajectory, and X_j^{start} and Y_j^{start} respectively represent the X and Y coordinates of the starting point of the jth trajectory. This study set a threshold $kCumulativeThresh_ = 2.05$ pixels to compare with the actual calculated population average displacement to determine whether there is significant systematic motion.

Standard deviation of displacement To measure the consistency of group movement, this study calculated the standard deviation of X-axis displacement (σ_x) and Y-axis displacement (σ_y) and compared them with the set threshold $kSdThresh_ = 0.23$. Firstly, calculate the average value of X-axis displacement (X) and Y-axis displacement (Y):

$$\bar{X} = \frac{1}{m} \sum_{j=1}^m X_j = \frac{1}{m} \sum_{j=1}^m (X_j^{end} - X_j^{start}) \quad (3)$$

$$\bar{Y} = \frac{1}{m} \sum_{j=1}^m Y_j = \frac{1}{m} \sum_{j=1}^m (Y_j^{end} - Y_j^{start}) \quad (4)$$

Then, calculate the standard deviation of X-axis displacement (σ_x) and Y-axis displacement (σ_y) according to the following formula:

$$\sigma_x = \sqrt{\frac{1}{m} \sum_{j=1}^m (X_j - \bar{X})^2} \quad (5)$$

$$\sigma_y = \sqrt{\frac{1}{m} \sum_{j=1}^m (Y_j - \bar{Y})^2} \quad (6)$$

Among them, $x_{(j)}$ and $y_{(j)}$ represent the displacement of the X axis and the displacement of the Y axis of the trajectory, respectively.

State decision matrix Based on the results of the trajectory displacement calculation, design a state decision matrix to determine the actual state of the vehicle's motion. The state decision matrix is based on the average displacement (Δd) and standard deviation (σ) of feature point displacements within the trajectory window. The specific classification criteria are as follows:

$$\text{Status} = \begin{cases} \text{Moving,} & \Delta dt > 2.05 \text{ px} \\ \text{Vibration,} & \Delta dt \leq 2.05 \text{ px} \wedge \sigma > 0.23 \text{ px} \\ \text{Static,} & \Delta dt \leq 2.05 \text{ px} \wedge \sigma \leq 0.23 \text{ px} \end{cases} \quad (7)$$

Using the decision matrix stated above and taking into account the different characteristics of vehicle motion, an accurate classification of vehicle motion states has been achieved. In practical applications, the matrix can be fine-tuned according to specific driving environments and vehicle characteristics.

4 Experimental Verification

4.1 Test Configuration

To evaluate the visual trajectory analysis scheme for commercial vehicle AEB systems, a dedicated dataset was constructed.

Dataset: The surge in learning-based methods has significantly increased the demand for diverse training data ([4]). Research ([29]) mentions that early studies explored pure camera-based methods under adverse conditions ([23,7]), but these methods used very small datasets, which are not suitable for commercial vehicle scenarios. Later, a series of multi-modal datasets ([20,21,32,10]) focused on noise issues. For example, the GGROUND dataset ([20]) emphasizes ground-penetrating radar localization under various weather conditions. The ApolloScape open dataset ([32]) combines LiDAR, camera, and GPS data, including scenarios with rainy conditions and bright scenes. The Ithaca365 dataset ([10]) is designed for the robustness of autonomous driving research, providing scenes under challenging weather conditions such as rain and snow. However, these datasets are not suitable for this study. Therefore, a dedicated dataset was created, composed of 32,454 video clips collected from 1,852 trucks, with each clip lasting 10 seconds. The dataset covers three motion states: static, vibration, and moving (slow and fast), including low-texture and high-texture road surface scenes. It covers various weather conditions, including sunny, overcast, and light rain, as well as changes in sunlight and shadows. This large-scale dataset covers most of the real-world scenarios encountered by commercial vehicles in operation. However, it does have some limitations, including insufficient extreme weather conditions, low video bitrate, and OSD interference.

4.2 Implementation Details

The motion detection system proposed in this study is based on a purely vision-based approach. The hardware platform utilizes the NVIDIA Jetson AGX Xavier ([19]) as the embedded computing unit. Table 2 provides the detailed hardware specifications of the system.

Table 2. Detailed hardware parameters

Device Type	Model/Parameters
Main Control Unit	Processor Intel(R) Core(TM) i9-14900KF 3.20 GHz
Main Control Unit	Onboard RAM 128 GB (128 GB available)
Main Control Unit	Storage 1.86 TB SSD GeIL P4A 2TB
Main Control Unit	Graphics Card NVIDIA GeForce RTX 4090 (24 GB)
Main Control Unit	System Type 64-bit Operating System, x64-based Processor
Vehicle Camera	APlus Blind Spot Camera, Uploaded Video is Compressed and Scaled

4.3 Results

Three types of classification results: As shown in Table 3, the Precision for the "moving" state reaches 99.985%, the F1-score is 98.205%, and the Recall is 96.486%. However, the "static" state has a Recall of 73.6%, with a Precision of only 65.151%, a Recall of 73.603%, and an F1-score of 69.12%. Similarly, the "vibration" state has a Recall of 69.708% and an F1-score of 69.497%. The relatively lower scores for the static and vibration states are mainly due to feature overlap between these two states in low-contrast scenarios.

The confusion matrix provides further insight into the specific classification performance of each category, as shown in Figure 4. A total of 3,926 static samples were correctly classified as static, but 1,408 were misclassified as vibration. This indicates that static and vibration states have similar features, making them prone to confusion.

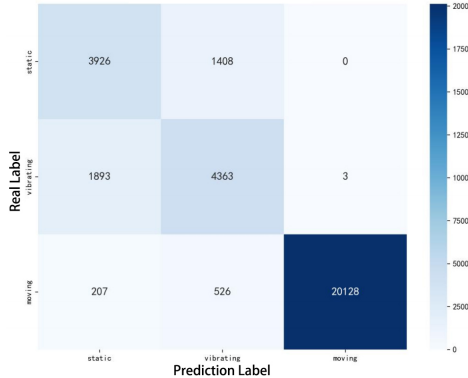


Fig. 4. Confusion matrix for classification of three types of motion states

Table 3. Performance analysis of three types of motion state classification details

State	Precision	Recall(Accuracy)	F1-score
Static	0.65151	0.73603	0.69120
Vibration	0.69287	0.69708	0.69497
Moving	0.99985	0.96486	0.98205

Two types of classification results: After merging the static and vibrating states into an unmoving state, we can observe from Table 4 that the Precision for the "unmoving" state reaches 94.092%, the F1-score is 96.923%, and the Recall is 99.974%. In the confusion matrix shown in Figure 4, the values for false

positives and false negatives are very low, indicating that the model performs exceptionally well in the binary classification task, particularly in applications that require high precision in determining "whether the vehicle is moving." Overall, the binary classification approach is more suitable for practical applications. However, to accurately detect the vibration state, future work will focus on optimizing CLAHE enhancement parameters, adjusting the ROI region, or introducing more complex models to improve the performance of the three-class classification.

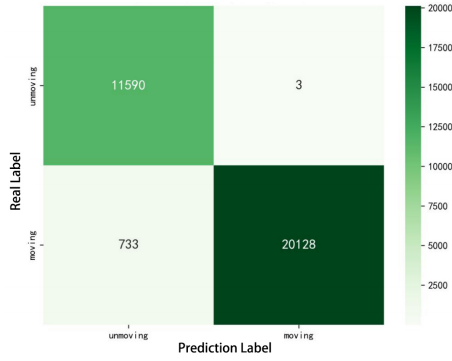


Fig. 5. Confusion matrix for classification of two types of motion states

Table 4. Performance analysis of two types of motion state classification details

State	Precision	Recall(Accuracy)	F1-score
unmoving	0.940 52	0.999 74	0.969 23
moving	0.999 85	0.964 86	0.982 05

Performance Testing: Performance testing evaluates the algorithm's processing efficiency by measuring latency and CPU utilization at different resolutions. The results are shown in Table 5.

From Table 5, it can be observed that at a resolution of 704×576 px, the algorithm's latency is 14.2 ± 1.3 milliseconds, with a CPU utilization of 9.8%. At a resolution of 1280×720 px, the latency increases to 22.7 ± 2.1 milliseconds, and the CPU utilization is 14.3%. This indicates that the algorithm can maintain low latency and low CPU utilization when processing images at different resolutions, demonstrating high processing efficiency.

In real-time vision processing tasks, low latency and high processing efficiency are key factors for ensuring system responsiveness. The algorithm proposed in

this study performs well in this regard, meeting the real-time requirements of commercial vehicle AEB systems.

Table 5. The relationship between resolution and system performance

Resolution (px)	latency (ms)	CPU Usage (%)
704×576	14.2(13)	9.8
1280×720	22.7(21)	14.3

4.4 Field Implementation

To validate the effectiveness of the vision-based trajectory analysis approach for zero-speed state detection in commercial vehicle AEB systems in real-world applications, we conducted a 6-month fleet test with 142 trucks. Before the test, the fleet frequently experienced braking errors due to inaccurate zero-speed detection, which impacted both transportation efficiency and safety. After deploying the system, the number of false braking events decreased by approximately 89%. This improvement is attributed to the algorithm's precise identification of the vehicle's motion state, preventing the AEB system from being falsely triggered when the vehicle is actually stationary or moving at low speeds.

During the testing period, when a vehicle suddenly braked or a pedestrian unexpectedly entered the roadway, the AEB system was able to trigger braking accurately and promptly. This demonstrated the reliability and effectiveness of the solution in real-world emergencies, ensuring the safety of both vehicles and pedestrians at critical moments.

Although the solution performed well in the overall testing, some failure cases still occurred. We conducted a detailed analysis of the causes of these failures and proposed corresponding mitigation strategies, as outlined in Table 6.

Table 6. Fault Frequency Mitigation Strategies

Mitigation Strategy	Fault Cause	Frequency
Sensor and wheel encoder fusion	Extremely low texture	2.1%
Activated rain removal algorithm	Heavy rainfall	1.7%
Adaptive exposure control	Sudden lighting change	1.2%

5 Discussion

5.1 Contribution

The main contributions of this study are as follows:

High-Precision Zero-Speed State Detection: This study introduces the SIFT-trajectory statistical method in the commercial vehicle zero-speed AEB scenario. By conducting a detailed analysis of the vehicle's motion trajectory, the method accurately distinguishes whether the vehicle is in a stationary or moving state, achieving a high detection accuracy of 99.97%. This effectively prevents false braking caused by misjudgment.

Effective Solution to the "0 km/h False Braking" Problem: In a practical test, the occurrence of false braking events was reduced by 89%. This demonstrates that the algorithm can accurately identify the vehicle's actual motion state, preventing the AEB system from being falsely triggered when the vehicle is stationary or moving at low speeds. This addresses the "0 km/h false braking" issue. In real-world applications, many commercial vehicles may experience rear-end collisions and other secondary accidents due to improper AEB system activation, which not only affects transportation efficiency but also endangers the driver's safety. The application of this algorithm can effectively reduce these risks and improve road transportation safety.

5.2 Limitations

During the practical testing, we identified several issues:

- 1. Insufficient Algorithm Robustness in Low-Texture and Extreme Weather Scenarios:** The algorithm's performance in environments with low texture or extreme weather conditions was not optimal, indicating the need for further improvements in these areas.
- 2. Confusion Between Static and Vibrating States:** There is still some confusion between the static and vibrating states, as the distinction between them is relatively low. However, for practical applications, the focus is primarily on differentiating between moving and non-moving states. Future work will delve deeper into addressing this issue.
- 3. Lack of Data for Extreme Weather Conditions:** The dataset used for testing lacks sufficient data for extreme weather scenarios. Future work will explore incorporating data from the Ithaca365 dataset [27] to include more extreme weather conditions for further training and refinement.

5.3 Future Work

Integrating Millimeter-Wave Radar to Enhance Performance in Rain and Fog: Although the method proposed in this study performs well in most environments, the performance of vision sensors may be impacted to some extent in adverse weather conditions such as heavy rain and fog ([37]). Radar technology has already been integrated into mass-produced vehicles for applications such as adaptive cruise control (ACC) and side-warning assistance ([17,30,27,13]). Therefore, considering the use of radar is essential. LiDAR is widely used in autonomous vehicles for obstacle detection ([24]); however, [11] suggests that normal rain and heavy rain may affect LiDAR performance. [35] highlights that

millimeter-wave radar has the advantage of being unaffected by weather conditions and accurately detecting the distance, speed, and angle of objects in harsh weather such as rain and fog. Future work will integrate millimeter-wave radar technology. By fusing data from visual sensors and millimeter-wave radar, the strengths of both can be fully utilized ([8,18]), improving the accuracy and reliability of vehicle state detection.

Developing an FPGA Accelerated Version: To meet the requirements of large-scale production and demonstrate the algorithm's processing efficiency and real-time performance, future work will also focus on developing a Field-Programmable Gate Array (FPGA) accelerated version. [1,12] shows that FPGA offers greater flexibility, shorter time-to-market, reliability, and maintainability. Additionally, an FPGA's powerful parallel processing capability can accelerate the hardware implementation of the algorithm, improving operational speed. By porting the algorithm to an FPGA platform, real-time processing can be achieved, ensuring that the AEB system can make correct decisions instantly.

In summary, the vision-based trajectory analysis algorithm for zero-speed state detection in commercial vehicle AEB systems proposed in this study offers significant advantages and broad application prospects. Through continuous optimization and improvement, this algorithm is expected to play an important role in the field of commercial vehicle safety, contributing to the safety and efficiency of road transportation.

6 Conclusion

The vision-based trajectory analysis algorithm for zero-speed state detection in commercial vehicle AEB systems proposed in this study aims to reduce the issue of "zero-speed braking" false triggers, improving the safety, comfort, and passenger protection in commercial vehicle operations. The algorithm integrates SIFT feature extraction with trajectory statistics, and through theoretical innovation and experimental validation, it has demonstrated a significant breakthrough in addressing the "zero-speed braking" false trigger problem. This algorithm shows substantial advantages and broad application prospects. With continuous optimization and improvement, it is expected to play a crucial role in the field of commercial vehicle safety, contributing to the safety and efficiency of road transportation.

Conflicts of Interest

The authors declare no conflicts of interest.

Funding

The authors received no financial support for the research, authorship, and/or publication of this article.

Data Availability Statement

The data that support the findings of this study are available from the corresponding author upon reasonable request.

References

1. Adams, L., Marketing, S.: Choosing the right architecture for real-time signal processing designs. Texas Instruments, Document Number SPRA879 (2002)
2. Ai, D., Han, X., Ruan, X., Chen, Y.W.: Adaptive color independent components based sift descriptors for image classification. In: 2010 20th International Conference on Pattern Recognition. pp. 2436–2439. IEEE (2010)
3. Amin, M.S., Reaz, M.B.I., Nasir, S.S., Bhuiyan, M.A.S., Ali, M.A.M.: A novel vehicle stationary detection utilizing map matching and imu sensors. The Scientific World Journal **2014**(1), 597180 (2014)
4. Arnold, E., Al-Jarrah, O.Y., Dianati, M., Fallah, S., Oxtoby, D., Mouzakitis, A.: A survey on 3d object detection methods for autonomous driving applications. IEEE Transactions on Intelligent Transportation Systems **20**(10), 3782–3795 (2019)
5. Atkins, W.: Research on the impacts of connected and autonomous vehicles (cavs) on traffic flow. Stage 2: Traffic modelling and analysis technical report (2016)
6. Burger, W., Burge, M.J.: Scale-invariant feature transform (sift). In: Digital Image Processing: An Algorithmic Introduction, pp. 709–763. Springer (2022)
7. Cai, B., Xu, X., Jia, K., Qing, C., Tao, D.: Dehazenet: An end-to-end system for single image haze removal. IEEE transactions on image processing **25**(11), 5187–5198 (2016)
8. Chavez-Garcia, R.O., Burlet, J., Vu, T.D., Aycard, O.: Frontal object perception using radar and mono-vision. In: 2012 IEEE Intelligent Vehicles Symposium. pp. 159–164. IEEE (2012)
9. Dhani, A.: Reported road casualties in Great Britain: Quarterly provisional estimates year ending September 2017. Technical report, U.K. Department for Transport, London, UK (Feb 2018), https://assets.publishing.service.gov.uk/government/uploads/system/uploads/attachment_data/file/681593/quarterly-estimates-july-to-september-2017.pdf
10. Diaz-Ruiz, C.A., Xia, Y., You, Y., Nino, J., Chen, J., Monica, J., Chen, X., Luo, K., Wang, Y., Emond, M., et al.: Ithaca365: Dataset and driving perception under repeated and challenging weather conditions. In: Proceedings of the IEEE/CVF Conference on Computer Vision and Pattern Recognition. pp. 21383–21392 (2022)
11. Fersch, T., Buhmann, A., Koelpin, A., Weigel, R.: The influence of rain on small aperture lidar sensors. In: 2016 German Microwave Conference (GeMiC). pp. 84–87. IEEE (2016)
12. Karim, M., El Kouache, M., Amarouch, M.Y., et al.: An fpga-based system for real-time electrocardiographic detection of stemi. In: 2016 2nd International Conference on Advanced Technologies for Signal and Image Processing (ATSIP). pp. 830–835. IEEE (2016)
13. Levinson, J., Askeland, J., Becker, J., Dolson, J., Held, D., Kammel, S., Kolter, J.Z., Langer, D., Pink, O., Pratt, V., et al.: Towards fully autonomous driving: Systems and algorithms. In: 2011 IEEE intelligent vehicles symposium (IV). pp. 163–168. IEEE (2011)

14. Li, L., Pan, Y., Lee, J.K., Ren, C., Liu, Y., Grejner-Brzezinska, D.A., Toth, C.K.: Cart-mounted geolocation system for unexploded ordnance with adaptive zupt assistance. *IEEE Transactions on Instrumentation and Measurement* **61**(4), 974–979 (2012)
15. Lowe, D.G.: Object recognition from local scale-invariant features. In: *Proceedings of the seventh IEEE international conference on computer vision*. vol. 2, pp. 1150–1157. Ieee (1999)
16. Lowe, D.G.: Distinctive image features from scale-invariant keypoints. *International journal of computer vision* **60**(2), 91–110 (2004)
17. Mao, X., Inoue, D., Kato, S., Kagami, M.: Amplitude-modulated laser radar for range and speed measurement in car applications. *IEEE Transactions on Intelligent Transportation Systems* **13**(1), 408–413 (2011)
18. Nishigaki, M., Rebhan, S., Einecke, N.: Vision-based lateral position improvement of radar detections. In: *2012 15th International IEEE Conference on Intelligent Transportation Systems*. pp. 90–97. IEEE (2012)
19. NVIDIA: *NVIDIA Jetson AGX Xavier*, <https://www.nvidia.com/eses/autonomous-machines/embedded-systems/jetson-agx-xavier/>
20. Ort, T., Gilitschenski, I., Rus, D.: Grounded: The localizing ground penetrating radar evaluation dataset. In: *Robotics: Science and Systems*. vol. 2 (2021)
21. Pitropov, M., Garcia, D.E., Rebello, J., Smart, M., Wang, C., Czarnecki, K., Waslander, S.: Canadian adverse driving conditions dataset. *The International Journal of Robotics Research* **40**(4-5), 681–690 (2021)
22. Robert Bosch GmbH: CAN Specification Version 2.0. Technical report, Robert Bosch GmbH, Stuttgart, Germany (1991)
23. Sakaridis, C., Dai, D., Van Gool, L.: Semantic foggy scene understanding with synthetic data. *International Journal of Computer Vision* **126**(9), 973–992 (2018)
24. Sato, S., Hashimoto, M., Takita, M., Takagi, K., Ogawa, T.: Multilayer lidar-based pedestrian tracking in urban environments. In: *2010 IEEE Intelligent Vehicles Symposium*. pp. 849–854. IEEE (2010)
25. Singh, M., Mishra, P., Aggarwal, N., Kumar, V., Sharma, P.K., Yadav, R.: Cosinerecom: A knn-based movie recommendation system using cosine similarity. In: *2024 4th International Conference on Advancement in Electronics & Communication Engineering (AECE)*. pp. 190–194. IEEE (2024)
26. Singh, S.: Traffic safety facts. Tech. Rep. DOT HS 812 115, Nat. Highway Traffic Saf. Admin., U.S. Dept. Transp, Washington, DC, USA (Feb 2015), <https://cras.hstats.nhtsa.dot.gov/Api/Public/ViewPublication/812115>
27. Sivaraman, S., Trivedi, M.M.: Looking at vehicles on the road: A survey of vision-based vehicle detection, tracking, and behavior analysis. *IEEE transactions on intelligent transportation systems* **14**(4), 1773–1795 (2013)
28. Skog, I., Handel, P., Nilsson, J.O., Rantakokko, J.: Zero-velocity detection—an algorithm evaluation. *IEEE transactions on biomedical engineering* **57**(11), 2657–2666 (2010)
29. Song, Z., Liu, L., Jia, F., Luo, Y., Jia, C., Zhang, G., Yang, L., Wang, L.: Robustness-aware 3d object detection in autonomous driving: A review and outlook. *IEEE Transactions on Intelligent Transportation Systems* (2024)
30. Tokoro, S., Kuroda, K., Kawakubo, A., Fujita, K., Fujinami, H.: Electronically scanned millimeter-wave radar for pre-crash safety and adaptive cruise control system. In: *IEEE IV2003 Intelligent Vehicles Symposium. Proceedings (Cat. No. 03TH8683)*. pp. 304–309. IEEE (2003)
31. Trombley, R.A., Pilutti, T.E.: False event suppression for collision avoidance systems (Feb 5 2013), uS Patent 8,370,056

32. Wang, P., Huang, X., Cheng, X., Zhou, D., Geng, Q., Yang, R.: The apolloscape open dataset for autonomous driving and its application. *IEEE transactions on pattern analysis and machine intelligence* **1** (2019)
33. Wang, S., Liu, Y., Li, D., Yan, H., Bai, B.: An improved sift feature extraction method for tyre tread patterns retrieval. In: 2014 Seventh international symposium on computational intelligence and design. vol. 1, pp. 539–543. IEEE (2014)
34. Wang, Y., Huang, Y., Peng, L., Wang, M., Li, W., Jing, M., Zeng, X.: S-sift: A simple sift algorithm with high efficiency. In: 2024 IEEE 17th International Conference on Solid-State & Integrated Circuit Technology (ICSICT). pp. 1–3. IEEE (2024)
35. Wenger, J.: Automotive mm-wave radar: Status and trends in system design and technology. In: IEE Colloquium on Automotive Radar and Navigation Techniques. pp. 1–1. IET (1998)
36. Zhang, H., Kong, D., Ao, G., et al.: Research progress of vehicle active collision prevention control technology. *High Tech. Lett.* **32**(3), 314–326 (2022)
37. Zhang, J., Zhang, Q., Hu, M., Tang, Y., Ma, G.: Research on verification and evaluation method of automatic emergency braking function in rain and fog weather based on topsis. In: 2024 10th International Conference on Control, Automation and Robotics (ICCAR). pp. 21–27. IEEE (2024)